Solute–solvent interactions in infinitely dilute supercritical mixtures: A molecular dynamics investigation

Irena B. Petsche and Pablo G. Debenedetti
Department of Chemical Engineering, Princeton University, Princeton, New Jersey 08544-5263

(Received 16 February 1989; accepted 23 August 1989)

A molecular dynamics investigation of the environment surrounding an infinitely dilute Xe-like Lennard-Jones atom in a supercritical Ne-like Lennard-Jones fluid shows enhanced solute–solvent interactions (clustering) in the vicinity of the solvent's critical point. Under near-critical conditions, the solute is at all times surrounded by an environment which is greatly enriched in solvent with respect to bulk conditions, but the identity of the solvent molecules in the cluster changes continuously. The enhancement of solute–solvent interactions in the Xe-in-Ne near-critical system is in contrast with the behavior exhibited by the symmetric Ne-in-Xe near-critical system (i.e., infinitely dilute Ne in near-critical Xe). In this case, the environment surrounding Ne atoms tends to be solvent lean with respect to bulk conditions. As Ne's critical point is approached, Ne–Xe interactions become progressively irrelevant with respect to Ne–Ne interactions, giving rise to pronounced density fluctuations around the Xe atoms. Differences between Xe-in-Ne and Ne-in-Xe near-critical systems are confirmed by cluster statistics and stability analysis.

INTRODUCTION

During the past five years, a number of experimental observations[1–5] and subsequent theoretical interpretations[3,6–9] have contributed towards an improved understanding of solute–solvent interactions in dilute supercritical mixtures. As a consequence, and although many important questions still remain unanswered, a consistent picture has gradually been emerging, the distinguishing feature of which is the establishment of a sound basis upon which a rigorous, molecular-based theory of supercritical mixtures can eventually be built.

Central to the recently gained insights into the nature of solute–solvent interactions in supercritical mixtures (and, paradoxically, also typical of the significant questions which still remain unanswered) is the concept of cluster formation. In the critical phenomena literature, it is customary to use the word cluster to denote a region of space in which order parameter fluctuations are correlated. In 1983, Eckert and co-workers[1] proposed the use of the same term to interpret their measurements of very large and negative partial molar volumes of dilute organic solutes in supercritical solvents (typically 2 orders of magnitude larger, in absolute value, than the solvent's bulk molar volume). These extraordinary volume contractions were interpreted by Eckert and co-workers in terms of the formation of solvent clusters around solute molecules; these investigators, furthermore, estimated the number of solvent molecules "bound" to each solute molecule from chemical theory arguments.[1] Although the divergence of the partial molar volume of an infinitely dilute solute at the solvent's critical point can be predicted by straightforward thermodynamic arguments,[10] the above observations and, in particular, the attempts at quantifying them in terms of an effective number of participating solvent molecules attracted the attention of numerous investigators.[3–9,11,12]

The introduction of trace amounts of a solute into a highly compressible solvent characterized by a diverging correlation length gives rise to cooperative behavior, the macroscopic manifestation of which is the singularity in the solute's partial molar properties. Recent experimental studies[3–5] have addressed the corresponding short-ranged behavior through the investigation of the local environment surrounding dilute solutes in supercritical solvents. Kim and Johnston[3] used solvatochromism (i.e., changes in the absorption wavelength of an indicator dye due to changes in the surrounding solvent environment) to probe the local environment around phenol blue in supercritical ethylene, fluoroform, and chlorotrifluoromethane. They found remarkable enhancements in solvent density around the dye probe. Subsequently, these authors[4] used the same technique to study the local environment around solute molecules in supercritical systems containing cosolvents; they found cosolvent enrichment around the phenol blue dye. Recently, Brennecke and Eckert[5] used fluorescence spectroscopy to study molecular interactions in highly dilute solutions of pyrene in supercritical carbon dioxide, ethylene, and fluoroform. Their experiments revealed enhanced solvent density around the pyrene probe in the vicinity of the solvent's critical point.

Recent theoretical work on solute–solvent interactions in dilute supercritical mixtures has focused primarily on long-ranged behavior.[6–9] Fluctuation theory was used[6] to derive a relationship between solute partial molar volumes at infinite dilution and cluster size, the latter quantity defined as the excess number of solvent molecules surrounding the infinitely dilute solute, with respect to a uniform distribution at bulk conditions. This fluctuation-based equation relating the above-defined cluster size to solute partial molar volume at infinite dilution is the quantitative substantiation of Eckert's proposed clustering mechanism; it shows that a diverg-

 0021-9606/89/237075-10$02.10 © 1989 American Institute of Physics

Downloaded 20 Jul 2006 to 128.112.35.75. Redistribution subject to AIP license or copyright, see http://jcp.aip.org/jcp/copyright.jsp

ing cluster size (long-ranged solvent enrichment around infinitely dilute solutes) is mathematically inseparable from the existence of large, negative solute partial molar volumes under near-critical, high compressibility conditions.

Starting from experimental[2] solute partial molar volume data, fluctuation theory-based calculations[6] yielded numbers as high as 110 excess solvent molecules per solute molecule for infinitely dilute tetrabromomethane in supercritical carbon dioxide. In addition, the fluctuation approach has been used to show the relationship between cluster formation, solubility enhancement,[6] and retrograde solubility[7] in dilute supercritical mixtures. It has also been shown[7] that, in near-critical systems, the divergence of the solvent's compressibility imposes asymptotic scaling laws whereby the cluster size and the solute's partial molar properties become proportional to each other, and all long-ranged effects occur on the same length scale, namely, that associated with the solvent's correlation length.

The possible behavior of binary near-critical mixtures (i.e., mixtures in which the solute is present in trace amounts and the solvent is near its critical point) has recently been classified into three categories[8]: attractive, weakly attractive, and repulsive. These regimes are characterized by the signs of the diverging solute partial molar volume and cluster size, which can be: negative, positive (attractive behavior), positive, negative (repulsive behavior), or positive, positive (weakly attractive behavior). In this context, a negative cluster (or cavity) is simply a region of space around the solute where the solvent's concentration is lower than in the bulk.

Recently, near-critical mixtures have been analyzed within the framework of integral equation theories.[9,11,12] Calculated pair correlation functions have shown that the growth in the cluster size (as defined above) is due to long-ranged correlations whereby deviations from bulk conditions due to the presence of a solute molecule persist over several molecular diameters. These theoretical developments[6–9,11,12] should be viewed within the context of the early pioneering work on the thermodynamics of near-critical mixtures by Krichevskii and his colleagues,[10,13] who used classical arguments, and of the illuminating non-classical treatments due to Wheeler[14] and to Levelt-Sengers and coworkers.[15–22]

Following the observation of highly negative solute partial molar volumes,[1–2] the concept of cluster formation was proposed[1] as a mechanistic explanation of these very large volume contractions upon solute addition. Subsequent experimental work has shown that, in addition to this long-ranged effect, a solute's immediate environment is strongly enriched with solvent (with respect to bulk conditions) in attractive near-critical mixtures.[3–5] Furthermore, theoretical treatments based on a definition of cluster size as the excess number of solvent molecules around an infinitely dilute solute molecule[6,7,10] yield very large numbers for this quantity, whose growth in the near-critical region can be related mathematically to macroscopically observable trends in the temperature and pressure dependence of the solubility of non-volatile solutes in supercritical solvents.[6,7]

Yet, despite the satisfying internal consistency of this picture, none of the above approaches, be they experimental or theoretical, has so far succeeded in answering basic questions, such as: What does a cluster look like? Are clusters stable, and therefore mechanistically significant objects, or are they merely mathematical objects of only statistical significance? What, if anything, do the experimental observations of strongly enhanced solute–solvent interactions in attractive near-critical mixtures imply as to the nature of the immediate environment surrounding solute molecules in such systems? How does this environment differ with respect to that which exists around the same solute molecule when immersed in the same solvent under conditions such that the latter is a dense liquid?

In this paper we investigate some of these questions through molecular-based computer simulations. Specifically, we study the structure and dynamics which characterize the local environment surrounding an infinitely dilute solute in a near-critical solvent, and we compare these results with those obtained upon interchanging solute and solvent. We also compare the local structure and dynamics with those that exist in the pure, near-critical solvent around randomly selected molecules.

The divergence of solute partial molar properties in infinitely dilute near-critical systems,[7] as well as the corresponding divergence of the cluster size (as defined within the context of fluctuation theory[6]) are universal phenomena, whose occurrence is quite independent of the chemical nature of the solute–solvent pair under consideration. In this sense, one can say that, as the solvent's critical point is approached, chemistry is reduced to a matter of signs, (i.e., whether solute partial molar properties diverge to $+\infty$ or $-\infty$; it is understood that we are talking here about nonreactive systems). The choice of model system to be simulated is therefore of secondary importance in this context, and we report here on the near-critical behavior of Lennard-Jones systems, which combine the all too infrequently paired virtues of relevance and simplicity.

The above considerations notwithstanding, it remains a fact that, in studying infinitely dilute near-critical systems via molecular dynamics, one obtains static and dynamic information on the local environment surrounding a test solute molecule. The behavior of this local environment, though influenced greatly by the proximity to the solvent's critical point (as will be shown), inevitably depends on the specific nature of the system under study to a greater extent than does the long-ranged behavior, the study of which is particularly ill suited to a molecular simulation approach. Accordingly, throughout the paper, we will distinguish those aspects that are general, and apply to all near-critical systems, from those that are specific to the mixture under study.

THE SYSTEMS

In this work, we compared the behavior of three systems: a pure fluid near its critical point, an infinitely dilute mixture of component α in near-critical β, and an infinitely dilute mixture of component β in near-critical α. Although we refer to atoms in the simulations as Ne or Xe, it should be understood throughout that this is only an approximation,

Downloaded 20 Jul 2006 to 128.112.35.75. Redistribution subject to AIP license or copyright, see http://jcp.aip.org/jcp/copyright.jsp

TABLE I. Mass, size[a,b] and energy[a,b] ratios for mixtures studied in this work.

	m_1/m_2	σ_1/σ_2	ϵ_1/ϵ_2
Mixture 1 [Xe(1) in Ne(2)]	6.506	1.435	7.04
Mixture 2 [Ne(1) in Xe(2)]	0.154	0.697	0.142

[a] $2\sigma_{12} = \sigma_1 + \sigma_2$; $\epsilon_{12} = (\epsilon_1\epsilon_2)^{1/2}$.
[b] Lennard-Jones parameters from viscosity data (Ref. 23).

TABLE II. State points investigated in this work.

State point	ρ^{*a}	T^{*b}
A	0.35	2
B	0.35	1.40
C	0.80	1.40

[a] $\rho^* = N\sigma^3/V$ (or $N\sigma_2^3/V$ in mixture simulations).
[b] $T^* = kT/\epsilon$ (or kT/ϵ_2 in mixture simulations).

insofar as we represent these substances through Lennard-Jones potentials, and we use Lorentz–Berthelot combining rules for Ne–Xe interactions.

Table I lists values of intermolecular potential parameters corresponding to the two binary systems studied here. Mixture 1 corresponds to the xenon (1; solute)–neon (2; solvent) system; mixture 2, to the neon (1; solute)–xenon (2; solvent) system. Every simulation was performed at constant temperature, volume, and number of particles (see the Appendix for technical details pertaining to the simulations). All binary simulations contained a single solute molecule and (N-1) solvent molecules, and they therefore provided information on the behavior of an infinitely dilute mixture obtained by changing the identity of a single solvent molecule in a pure solvent at fixed temperature and volume.

Within the context of the van der Waals theory of mixtures, mixture 1 (Xe in Ne) is predicted to exhibit attractive behavior (solvent enrichment around the solute) in the near critical region[8] (see the Appendix for calculations). Similarly, the theory predicts that, upon interchanging solute and solvent (i.e., the infinitely dilute solute becomes the near-critical solvent and vice–versa), the system (Ne in Xe) will exhibit repulsive behavior. We henceforth refer to mixture 1 (Xe in Ne) as attractive, and to mixture 2 (Ne in Xe), as repulsive. Note that we invoke the van der Waals theory[8] only to predict attractive or repulsive behavior, and not to quantify the growth of the solvent-rich or solvent-lean regions around the solute in the near-critical region. The latter type of question cannot, of course, be answered accurately by a classical equation of state.

The distinction between attractive and repulsive behavior is of fundamental importance in the near-critical region. In particular, all of the actual or proposed applications of supercritical fluids to processes ranging from crystallization[24] to precipitation polymerization[25] involve attractive behavior. Furthermore, we recognize the experimental observations of Eckert, Johnston, and co-workers,[1-5] and, in particular, the phenomenon commonly referred to as clustering, as manifestations of near-critical attractive behavior.

We now seek a detailed picture of the structural and dynamic characteristics of the local environment surrounding solutes in model attractive and repulsive near-critical systems via molecular dynamics.

FLUID STRUCTURE: PAIR CORRELATION FUNCTIONS

Table II shows the density–temperature coordinates of the state points explored in this study. Note that path $A \rightarrow B$ represents an isochoric quench into the Lennard-Jonesium's near-critical region ($\rho_c^* = N\sigma^3/V \cong 0.35; T_c^* = kT/\epsilon \cong 1.35$),[26] and $B \rightarrow C$ represents an isothermal compression at a slightly supercritical temperature.

At each state point, we performed three different simulations: 864 identical Lennard-Jones atoms; 863 identical Lennard-Jones solvent atoms plus one Lennard-Jones solute, with $\sigma_1/\sigma_2 = 1.435$, $\epsilon_1/\epsilon_2 = 7.04$, $m_1/m_2 = 6.506$ (Xe in Ne; attractive mixture; Table I); 863 identical Lennard-Jones solvent atoms plus one Lennard-Jones solute, with $\sigma_1/\sigma_2 = 0.697$, $\epsilon_1/\epsilon_2 = 0.142$, $m_1/m_2 = 0.154$ (Ne in Xe; repulsive mixture; Table I). Since there is but one Lennard-Jones fluid, the pure system represented both Ne (for comparisons with attractive mixture simulations) and Xe (for comparisons with repulsive mixture simulations). In all cases, units were scaled with solvent quantities (i.e., in the attractive mixture, for example, the solute's size was 1.435, and, in the repulsive mixture, 0.697). The selection of an adequate system size for simulations at state point B is discussed in the Appendix. Here, we simply mention the fact that the solvent pair correlation function (g_{22}) obtained from the binary simulations at state point (B) was indistinguishable from the pure component pair correlation function, thus guaranteeing that the system is large enough as to accommodate the solute and still remain near critical.

Figure 1 shows the solvent–solvent pair correlation function (g_{22}) for the pure (P) system, and the solute–solvent pair correlation functions (g_{21}) for the infinitely dilute attractive (A) and repulsive (R) mixtures at state point A ($T^* = 2, \rho^* = 0.35$). The corresponding pure and attractive

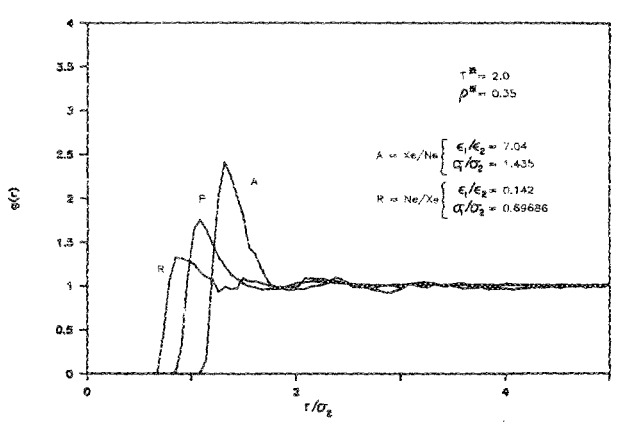

FIG. 1. Pair correlation functions for the pure system (P), attractive (A), and repulsive (R) mixtures at $T^* = 2, \rho^* = 0.35$ (1 = solute; 2 = solvent). All curves are averages over 5500 snapshots in the course of 15 000-step simulations of 864 atoms.

Downloaded 20 Jul 2006 to 128.112.35.75. Redistribution subject to AIP license or copyright, see http://jcp.aip.org/jcp/copyright.jsp

functions are shown in Fig. 2, for the near-critical state point B, at the same density ($T^* = 1.4, \rho^* = 0.35$). Although an increase in the height of the first peak upon cooling is to be expected, the attractive mixture exhibits a much more pronounced increase in this quantity than the pure system. In fact, at these near-critical conditions, each Xe atom is surrounded by an environment significantly enriched in Ne with respect to bulk conditions. The local Ne density 3.72 Å away from the Xe atom is 3.86 times higher than in the bulk. This pronounced solvent enrichment in the solute's immediate environment is precisely what is measured in solvatochromic,[3,4] and fluorescence spectroscopy[5] investigations of dilute supercritical mixtures.

The solvent–solvent correlation function (curve P, Fig. 2) decays to unity only at $6\sigma_2$. For $N = 864$ and $\rho^* = 0.35$, the computational box size, L, equals 13.52 σ_2. This means that correlations, though long ranged, do not exceed $L/2$ (away from the critical point, this condition is satisfied with much smaller system sizes). In this study, we simulate infinite dilution by using a single solute molecule. This imposes limitations on the statistical significance of calculated long-ranged correlations (as can be seen from the noise in the curves labeled A and R beyond their respective first peaks, Fig. 1). Nevertheless, the attractive correlation function definitely shows a very slow decay. Except for a very shallow first valley (minimum $g_{12} = 0.97$, at a distance 5.53 Å away from the Xe atom), the curve is consistently above unity throughout the range between 5.67 and 10.97 Å (or, equivalently, between 2.01 and 3.89 effective Ne diameters). These long-ranged effects are shown in detail in Fig. 3.

The corresponding behavior for the repulsive mixture is shown in Fig. 4. Each curve is an average over 5000 snapshots, and spans an interval of 22.1 ps. The environment surrounding the Ne atom fluctuates continuously, exhibiting the long-ranged solvent depletion predicted by the van der Waals theory[8] as well as temporary solvent enrichment. This interesting dynamic behavior is not to be found in the attractive case. Although the limitations of a purely energetic interpretation of near-critical behavior have already been

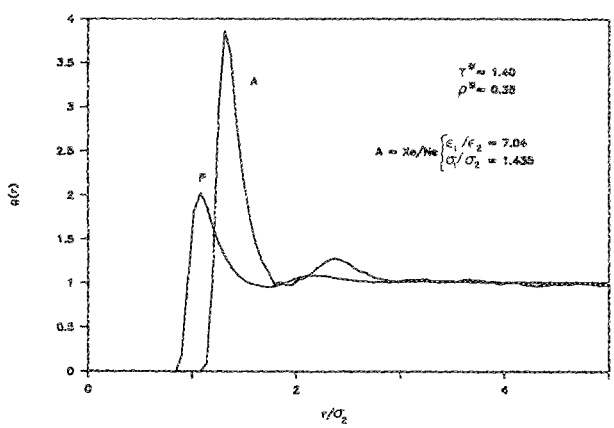

FIG. 2. Pair correlation functions for the pure (P) and attractive (A) systems at $T^* = 1.4, \rho^* = 0.35$ (1 = solute; 2 = solvent). The pure and attractive curves are averages over 6000 and 15 000 snapshots, respectively, in the course 15 000-step simulations of 864 atoms.

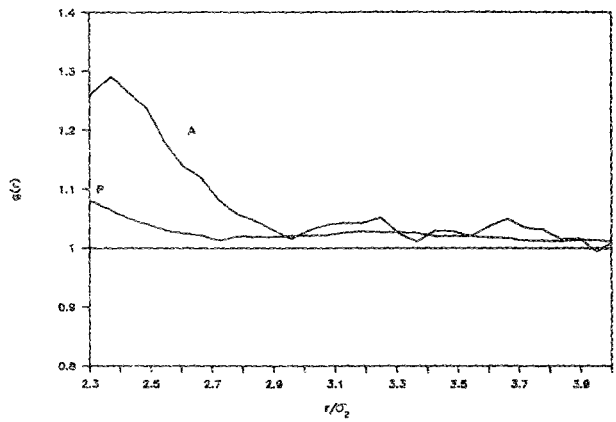

FIG. 3. Long-ranged tails of the attractive (A) and pure (P) pair correlation functions corresponding to Fig. 2.

pointed out[8] one can, in principle, rationalize the difference between attractive and repulsive behavior by noting that, in the former case, Xe–Ne interactions have a well depth 2.65 times larger than Ne–Ne interactions (1–2 interactions favored); in the latter case (2–2 interactions favored), the solvent–solvent (Xe–Xe) well depth is 2.65 times greater than the corresponding solute–solvent (Ne–Xe) value (Fig. 5).

The solvent depletion around the solute in the case of

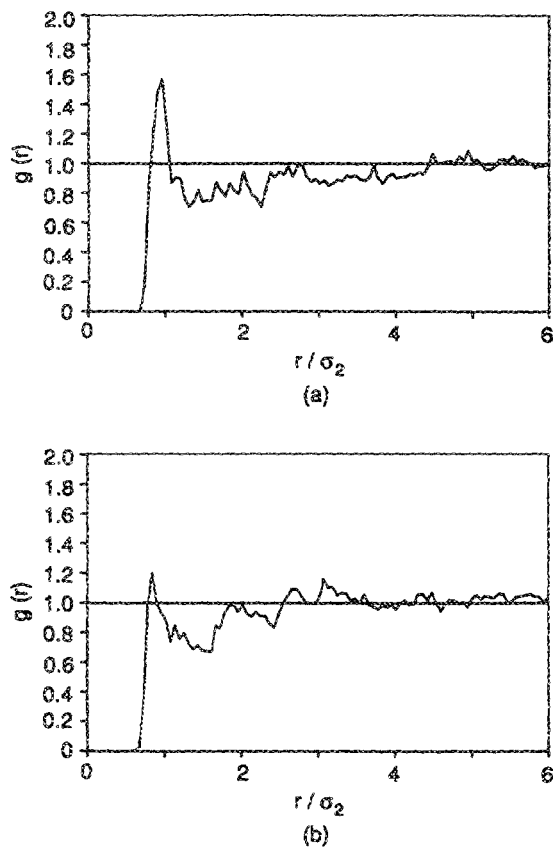

FIG. 4. Pair correlation functions for the repulsive mixture at $T^* = 1.4$, $\rho^* = 0.35$ (1 = solute; 2 = solvent $\sigma_1/\sigma_2 = 0.697$; $\epsilon_1/\epsilon_2 = 0.142$). Each curve is an average over 5000 steps, spanning 22.1 ps. The noise is indicative of weakened solute–solvent interactions and enhanced density fluctuations near the solvent's critical point. $N = 864$.

Downloaded 20 Jul 2006 to 128.112.35.75. Redistribution subject to AIP license or copyright, see http://jcp.aip.org/jcp/copyright.jsp

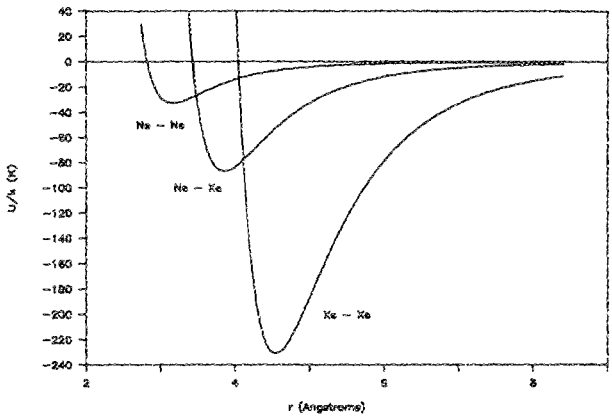

FIG. 5. Lennard-Jones representation of Xe–Xe, Ne–Ne, and Xe–Ne pair potentials, with parameters as per Table I. k is Boltzmann's constant.

repulsive behavior is thus seen to be a consequence of enhanced solvent interactions with respect to solute–solvent interactions. Since attractive interactions are enhanced in a compressible solvent,[3,4] the behavior shown in Fig. 4, which is indicative of pronounced solvent density fluctuations, is only to be found in the near-critical region. In a repulsive near-critical mixture, therefore, the environment surrounding solute molecules is largely dominated by solvent interactions (and, therefore, by pronounced solvent density fluctuations); in an attractive near-critical system, solute–solvent interactions are dominant.

From a purely computational viewpoint, one concludes from Figs. 2 and 4 that it is much more difficult to gather statistics on solute–solvent correlations in repulsive near-critical systems than it is for their attractive counterparts, since solute–solvent interactions become progressively irrelevant in the former case (and important in the latter case) as the critical point is approached. In this sense, the noise which characterizes each of the curves in Fig. 4 is qualitatively similar to that which one finds when calculating pair correlation functions in very dilute systems.

Upon compressing isothermally to point C ($T^* = 1.4$, $\rho^* = 0.8$), we recover the distribution functions shown in Fig. 6. We note, in the first place, a decrease in the attractive peak (from 3.86 at state point B to 2.98 at state point C). Thus, as the mixture is compressed away from the near-critical region, the solvent enrichment around the solute (with respect to bulk conditions) is progressively weakened. Conversely, in the case of the repulsive mixture, the decrease in the solvent's compressibility leads to an increase in the first peak, and to a pronounced decrease in the statistical uncertainties (noise) of the pair correlation function beyond the first peak. This means that solute–solvent interactions are enhanced away from criticality for repulsive mixtures. In both cases, therefore, we see enhanced attractive interactions in a highly compressible, near-critical solvent.[3,4] As for the pure system, we see that long-ranged behavior disappears, and is replaced by the oscillatory pattern characteristic of dense liquids.

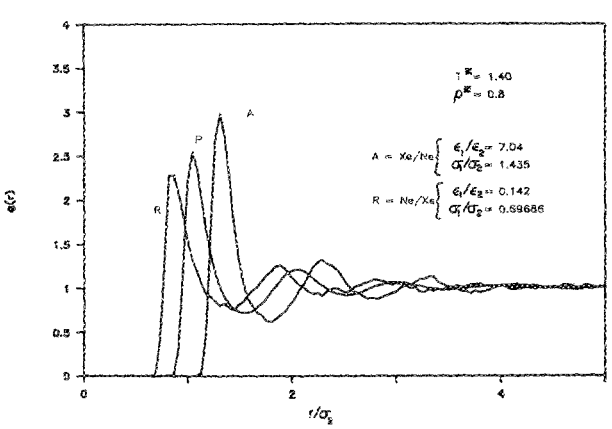

FIG. 6. Pair correlation functions for the pure system (P), attractive (A), and repulsive (R) mixtures at $T^* = 1.4$, $\rho^* = 0.8$ (1 = solute; 2 = solvent). All curves are averages over 5500 snapshots in the course of 15 000-step simulations of 864 atoms.

CLUSTER FORMATION

The pair correlation functions describe the fluid's structure in a time-averaged, statistical sense. We now turn our attention to the shape, size, and stability of molecular aggregates (or clusters, as they will henceforth be called) in the near-critical region. The use of the word cluster in the present context should not be confused with the fluctuation-theory-based definition of a cluster[6-8] as the excess number of solvent molecules surrounding a given solute molecule, at infinite dilution, with respect to a uniform distribution at the prevailing bulk density.

In discussing clusters one needs, in the first place, an unambiguous definition of such entities. As pointed out originally by Hill,[27] such a definition is arbitrary, although one expects "reasonable definitions to converge on the same predictions." In this work, we consider two types of clusters, which we define according to energetic and geometric criteria, respectively. In the former case, we consider two molecules i and j to be bound if their relative kinetic energy is smaller than $-\phi_{ij}$ (pair potential), and not "bound" either if $\phi_{ij} > 0$, or if their relative kinetic energy exceeds $-\phi_{ij}$.[27] The relative kinetic energy of two molecules having velocities $\mathbf{v}_i$ and $\mathbf{v}_j$ is given by

$$EK_{\text{rel}} = \frac{1}{2}\frac{m_i m_j}{m_i + m_j}(\mathbf{v}_i - \mathbf{v}_j)\cdot(\mathbf{v}_i - \mathbf{v}_j) \tag{1}$$

and is related to the total kinetic energy by

$$EK_{\text{tot}} = EK_{\text{rel}} + \frac{m_i + m_j}{2} V\cdot V, \tag{2}$$

$$(m_i + m_j)V = m_i\mathbf{v}_i + m_j\mathbf{v}_j, \tag{3}$$

where the second term in Eq. (2) is the center-of-mass kinetic energy.

As for a geometrically defined cluster, we are concerned here with the number of molecules contained within a specified distance from a "central" molecule, in the spirit of solvatochromic and fluorescence spectroscopy investigations of the solvation environment surrounding dilute solutes in supercritical solvents.[3-5]

Except for the above definition, in which we are only interested in counting neighbors around a specified "nucleus," molecules can, in general, be bound to other mole-

Downloaded 20 Jul 2006 to 128.112.35.75. Redistribution subject to AIP license or copyright, see http://jcp.aip.org/jcp/copyright.jsp

cules in the cluster (whether energetically or geometrically) either directly or indirectly. Directly bound particles are simply those pairs which satisfy the energetic criterion defined above (or an alternative geometric cutoff criterion); indirectly bound particles are connected through intermediate members of the cluster. Thus, particles α, β, and γ, in which α and β are directly bound to γ but not to each other, constitute a triplet (Fig. 7). It is obvious that accounting for indirectly connected members of a cluster calls for an efficient algorithm. In this work, we computed the statistics relevant to energetically defined clusters by implementing the elegant approach recently proposed by Sevick *et al.*[28]

Throughout this work, therefore, energetically defined clusters include indirectly bound particles, whereas geometrically defined clusters are entities composed of particles surrounding a specified nucleus. We do not consider geometrically defined clusters which include indirectly bound particles.

Figure 8 shows the cumulative relative frequency of occurrence of energetically defined clusters at state point B, for the attractive, repulsive, and pure systems. In the mixture cases, only those clusters which include the single solute are considered (by definition, there can be at most one such cluster at any instant). The reported cluster sizes include the solute, therefore a cluster size of 1 indicates that there are no solvent particles in the cluster [i.e., no particle bound to the solute (mixture case) or the randomly selected solvent atom (pure case)]. Figure 8 illustrates the distribution of cluster sizes observed over 5000 equally spaced snapshots in the course of 50 000 step simulations (see the Appendix for technical details). All distributions converged to their "true" values (i.e., the curves shown in Fig. 8) within less than 5000 snapshots. This is best illustrated by the evolution of the calculated mean cluster size, which converged to its final value of 3 (repulsive mixture), 16 (pure fluid), and 75 (attractive mixture) after 2000 snapshots (repulsive mixture), 4000 snapshots (pure fluid), and 3000 snapshots (attractive mixture). In all cases, cumulative distribution curves obtained after 4000 and 5000 snapshots were superimposable.

The cluster distributions shown in Fig. 8 are very different from each other. The repulsive mixture (Ne in Xe) exhibited a cluster size of 1 (no Xe atom bound to the Ne probe) 89.98% of the time, and dimers, 2.38% of the time. The curvature of the distribution shows that larger clusters occurred with decreasing frequency: clusters involving more than five atoms (including the Ne probe) accounted for only 5.18% of the observations. The pure near-critical solvent exhibited a cluster size of 1 (no atom bound to the randomly selected probe) 36.98% of the time, and dimers, 12.62% of the time. The curvature of the distribution indicates, as in the repulsive case, a monotonically decreasing frequency of occurrence as the cluster size increases. Clusters involving more than five atoms (including the randomly selected probe) accounted for 35.54% of the observations, and the median cluster size (cumulative relative frequency = 0.5) was 2. By contrast, the attractive mixture (Xe in Ne) exhibited a very different distribution. The cumulative frequency curve has vanishing slope at the origin (unbound probe never observed), and maximum slope for cluster sizes between 20 and 40 (clusters within this size range occurred most frequently), indicating a frequency distribution that is not monotonically decreasing. Dimers occurred only 0.088% of the time, and clusters involving more than five atoms (including the Xe probe) accounted for 99.52% of all observations. The median cluster was 59.

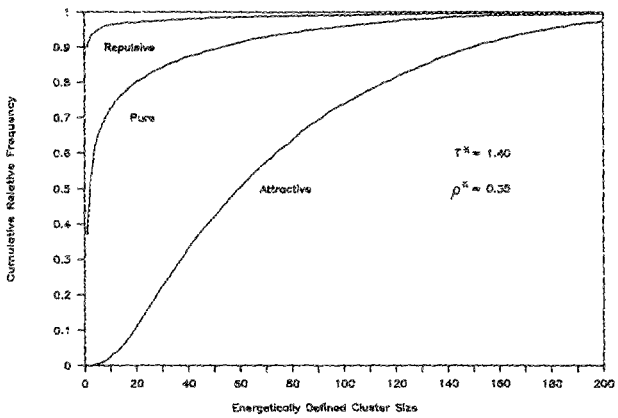

FIG. 8. Cumulative relative frequency of occurrence of energetically defined clusters surrounding the Xe atom (attractive mixture), the Ne atom (repulsive mixture), and a randomly chosen atom (pure system) at $T^* = 1.4, \rho^* = 0.35$. Each curve was obtained by computing the cluster size at 5000 equally spaced snapshots in the course of 50 000 step simulations of 864 atoms. For a given abscissa value (n), the ordinate is the sum over all clusters of size $\leqslant n$ of the number of times such clusters were observed, divided by the total number of snapshots.

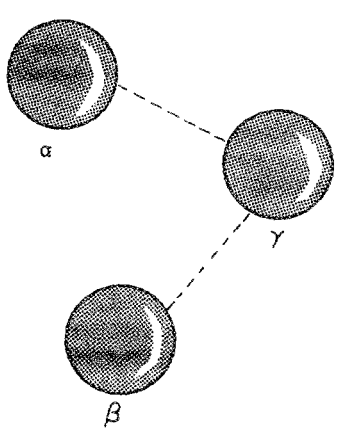

FIG. 7. A triplet in which particles α and β are directly bound to γ but not to each other.

It is interesting to compare the stability (i.e., persistence in time) of energetically defined near-critical clusters in the pure and attractive cases. This is done in Fig. 9, in which the y axis gives the percentage of particles belonging to a particular cluster at time t which also belonged to the same cluster at time 0 (i.e., we measure the time it takes for a cluster to lose its identity, but not necessarily its structural integrity). Initial cluster sizes were 100 (pure) and 102 (attractive) particles, respectively. Figure 9 is representative of many similar observations. As explained above, an energetically defined cluster includes indirectly bound atoms; it is hence highly branched, and the breaking of one pair of bound particles

Downloaded 20 Jul 2006 to 128.112.35.75. Redistribution subject to AIP license or copyright, see http://jcp.aip.org/jcp/copyright.jsp

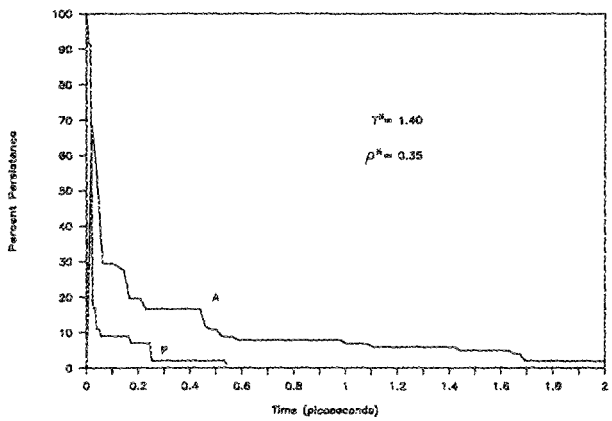

FIG. 9. Identity persistence of energetically defined clusters at $T^* = 1.4$, $\rho^* = 0.35$. The vertical axis gives the percentage of particles belonging to an energetically defined cluster at time t which also belonged to the cluster at time 0. The pure cluster (P) consisted, initially, of 100 Ne atoms; the attractive (A) cluster, of 102 Ne atoms and a Xe nucleus.

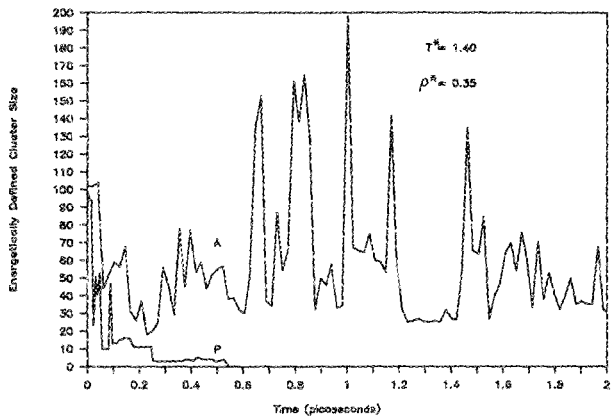

FIG. 10. Cluster sizes corresponding to Fig. 9. The pure cluster disappears, whereas the Xe atom is at all times surrounded by an energetically defined cluster of changing identity.

causes the loss of all other particles connected to the unbound particle. The initial rapid decay of both curves reflects this loss of identity at the periphery, the effect of the solute being important only in the environment closely surrounding it. Thus it is the total decay time which distinguishes the two types of systems (pure solvent, attractive mixture).

In order to quantify differences in persistence times, we tracked the evolution of clusters containing 60 or more particles for both the pure and attractive systems in the course of 50 000 step simulations. In the former case, 54 clusters were tracked; in the latter, 142 [recall that clusters of 60 or more particles accounted for 8.66% of the observations for the pure solvent (Fig. 8), while for the attractive system they accounted for 49.58% of the observations]. Neither the attractive nor the pure system exhibited any correlation whatsoever between cluster size and decay time (when results were plotted as decay time vs initial cluster size, data points were randomly scattered). This important observation means that the lifetime of an energetically defined cluster is indicative of the time it takes to renew the identity of particles located in the environment closely surrounding the nucleus. For the pure system, the shortest observed decay time was 0.016 ps; the longest, 1.76 ps. The average time for a pure cluster to lose its identity was 0.54 ps, but with a standard deviation of 0.39 ps. For the attractive system, the shortest decay time was 0.44 ps, while 94 of the 142 observations (i.e., 66.2% of the total) exceeded the maximum tracking time of 2.09 ps (this limitation being imposed by the considerable time consumption of the cluster tracking algorithm). The average time for an attractive cluster to lose its identity was found to be greater than 1.88 ps, with a standard deviation of 0.37 ps (clusters which did not decay by 2.09 ps were assigned a decay time of 2.09 seconds): note that this conservative calculation yields an average time 3.48 times greater than in the corresponding pure case.

Shown in Fig. 10 are instantaneous cluster sizes corresponding to Fig. 9. Note that the pure cluster disappears while the attractive cluster is typically in the 20 to 60 size range. As discussed above, the type of clusters whose evolution is tracked in Figs. 9 and 10 include particles indirectly bound to the nucleus (solute or randomly chosen solvent). This means that the breaking of one bond results in the loss of an entire branch while the creation of a single bond attaches an entire branch. This is the origin of the fluctuations in cluster size shown in Fig. 10. These results, which are typical of many similar observations, show that, whereas the Xe atom is always surrounded by a large (energetically defined) cluster of near-critical Ne, the corresponding large clusters of pure Ne in the vicinity of its critical point are constantly being formed and destroyed. The irreversible decay of curve A in Fig. 9 is therefore indicative of a change in the identity of the environment closely surrounding the Xe "impurity."

As mentioned before, experimental studies aimed at understanding molecular interactions in dilute supercritical mixtures[3–5] provide information on the immediate environment surrounding solute molecules in such systems. Kim and Johnston's observations[3,4] (as well as Brennecke and Eckert's[5]) suggest a remarkable solvent enrichment around the solute (only attractive systems were studied), in agreement with the behavior of the first peak of g_{12} shown in Fig. 2 (curve A). We now examine the immediate environment surrounding infinitely dilute solutes in attractive and repulsive near-critical mixtures in greater detail. To this end, we adopt a purely geometric definition of a cluster in which we are only interested in counting molecules within a certain separation from a given nucleus. It is clear that, when such a nucleus is the solute, we recover information of the type obtained in solvatochromic experiments, albeit with much greater detail concerning the motion of individual molecules, as is always the case in molecular-based computer simulations.

Figure 11 is a typical snapshot of the 39 nearest neighbors surrounding a randomly selected atom in the course of a simulation of the pure Lennard-Jonesium at state point B. The remaining 824 atoms in the simulation are not shown. The maximum distance between the nucleus and one of its 39 nearest neighbors is 8.24 Å (solvent represents Ne; comparison with attractive mixture), or 11.82 Å (solvent represents Xe; comparison with repulsive mixture). Figure 12 shows a typical snapshot of the 39 nearest neighbors surrounding the

Downloaded 20 Jul 2006 to 128.112.35.75. Redistribution subject to AIP license or copyright, see http://jcp.aip.org/jcp/copyright.jsp

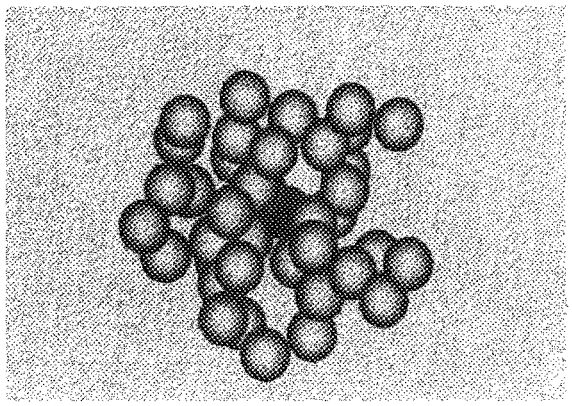

FIG. 11. Instantaneous configuration of the 39 nearest neighbors surrounding a randomly selected atom (black) of a pure Lennard-Jonesium at $T^* = 1.4, \rho^* = 0.35$.

Xe atom in near-critical Ne (state point B). The remaining 824 atoms in the simulation are not shown. The separation between the Xe nucleus and the most distant among the Ne neighbors shown in Fig. 12 is 7.21 Å. It is evident from Figs. 11 and 12 (both of which are typical of many similar observations and correspond to the same bulk density) that the introduction of a Xe atom in near-critical Ne causes a remarkable solvent enrichment around the solute. The same information, but this time for the repulsive mixture, is shown in Fig. 13. In this case, the solute is Ne, and the solvent, Xe (the solvent has constant, unit size in Figs. 11–13). The solvent depletion around the solute is evident. The separation between the Ne nucleus and the most distant among its 39 nearest neighbors is now 12.83 Å.

Figure 14 shows the evolution in time of the solute–solvent distance corresponding to the five closest Ne neighbors around the Xe atom during a typical interval of 10 ps in the course of a simulation at state point B. Curves are labeled in order of ascending Xe–Ne separation at time 0. The effective diameter for Xe–Ne interactions [i.e., $(\sigma_1 + \sigma_2)/2$] is 3.43 Å. At time 0, the closest Ne atom is 3.46 Å away from the Xe nucleus, whereas atom 5 is 3.77 Å away (the first peak in g_{12}, Fig. 2, occurs 3.72 Å away from the Xe atom). After 4 ps, two out of the five nearest neighbors are still

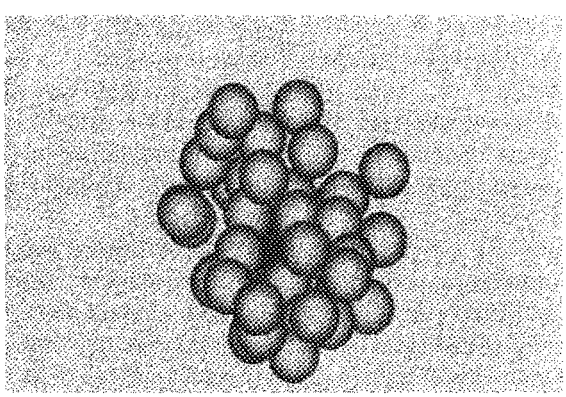

FIG. 12. Instantaneous configuration of the 39 nearest Ne neighbors surrounding the Xe atom (black) at the same temperature and number density as in Fig. 11. Note the solvent enrichment around the solute. $\sigma_1 = 1.435$; $\sigma_2 = 1$.

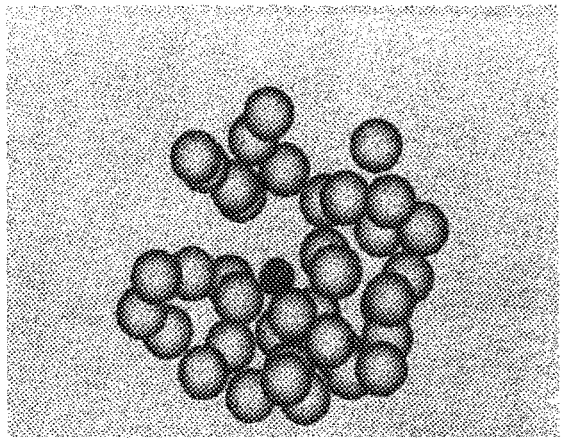

FIG. 13. Instantaneous configuration of the 39 nearest Xe neighbors surrounding the Ne atom (black) at the same near-critical conditions as in Fig. 11. Note the solvent depletion around the solute. $\sigma_1 = 0.697$; $\sigma_2 = 1$.

within the first g_{12} peak. After 7.4 ps, the five nearest neighbors have moved beyond 2 Ne diameters away from the Xe atom (i.e., past the first valley in g_{12}).

Figure 15 shows the corresponding behavior for the five closest Ne atoms around the randomly selected Ne nucleus in the course of a simulation at state point B. The effective diameter for Ne–Ne interactions is 2.82 Å. At time 0, the closest Ne atom is 3.32 Å away from the Ne nucleus, whereas atom 5 is 5.57 Å away (the first peak in g_{22}, Fig. 2, occurs at a Ne–Ne distance of 3.05 Å, and the first valley, at 4.9 Å). This difference in the initial separations with respect to Fig. 14, where the five closest Ne atoms were within 3.77 Å of the Xe nucleus is, of course, consistent with the pronounced solvent enrichment around the solute shown in Fig. 12. After 4 ps, four out of five nearest neighbors have moved more than 3 Ne diameters away from the nucleus.

Attractive clusters, therefore, preserve their identity over longer periods of time than their pure counterparts, just as was found to be the case with energetically defined clusters. In addition, attractive near-critical clusters renew their identity continuously, but this process takes place without

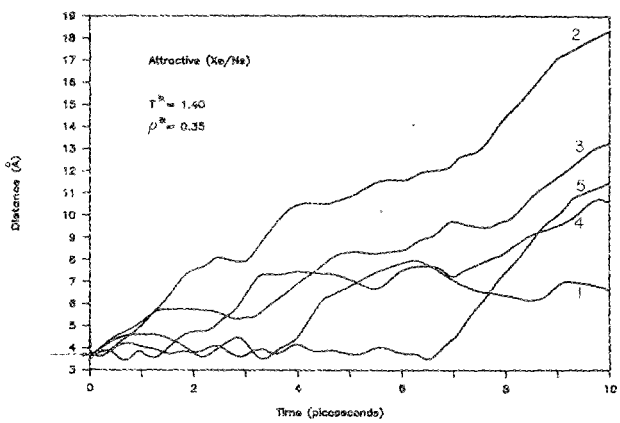

FIG. 14. Time dependence of solute–solvent distance corresponding to the five closest Ne neighbors surrounding the Xe atom at $T^* = 1.4, \rho^* = 0.35$. Curves are labeled in order of increasing Xe-Ne separation at time 0. Arrow in the vertical axis indicates the location of the first peak in the attractive pair correlation function (Fig. 2).

Downloaded 20 Jul 2006 to 128.112.35.75. Redistribution subject to AIP license or copyright, see http://jcp.aip.org/jcp/copyright.jsp

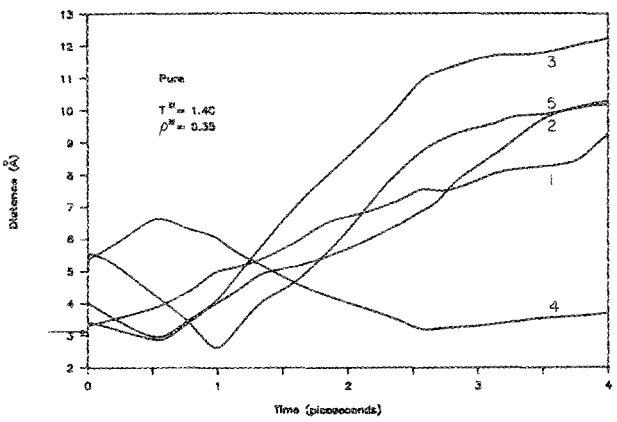

FIG. 15. Time dependence of the solvent–solvent distance corresponding to the five closest Ne neighbors surrounding a randomly selected Ne atom at $T^* = 1.4, \rho^* = 0.35$. Curves are labeled in order of increasing Ne–Ne separation at time 0. Arrow in the vertical axis indicates the location of the first peak in the pure pair correlation function (Fig. 2).

disruption of the solvent-rich environment around the solute (Fig. 12). By contrast, clusters in a pure near-critical solvent not only renew their identity continuously, but are constantly being formed and destroyed around any randomly chosen solvent molecule (this, of course, is to be expected from the fact that all solvent molecules are identical).

CONCLUSION

Molecular dynamics simulations of a model atomic system in which $\epsilon_{12} > \epsilon_2$ (1 = solute; 2 = solvent) exhibit a pronounced solvent enrichment around the infinitely dilute solute atoms in the vicinity of the solvent's critical point. This solvent-rich environment tends to preserve its structural integrity, though not its identity. If, on the other hand, $\epsilon_{12} < \epsilon_2$ (a condition which, in this study, was attained by interchanging solute and solvent), the environment around the infinitely dilute solute tends to be solvent lean with respect to bulk conditions as the solvent's critical point is approached. In this case, there is no characteristic solvent structure around the solute, whose environment undergoes pronounced density fluctuations. Both types of behavior are consistent with an enhancement of attractive interactions in highly compressible solvents.

Because dilute near-critical mixtures behave in one of three possible ways[8] (attractive, weakly attractive, repulsive), the present study is relevant to the interpretation of recent solvatochromic[3,4] and fluorescence spectroscopy[5] studies of attractive mixtures of dilute organic solutes in supercritical solvents, which showed strongly enhanced solute–solvent interactions in the critical region. The simulation results suggest that the proposed clustering picture[1] is indeed mechanistically significant in the vicinity of solute molecules, where a very compact, solvent-rich aggregate is at all times present.

ACKNOWLEDGMENTS

The authors gratefully acknowledge the financial support of the National Science Foundation (Graduate Fellowship Award to IBP; Presidential Young Investigator Award CBT—8657010 to PGD). All simulations were performed on Cyber 205 and ETA-10 machines located at the John von Neumann National Supercomputer Center, in Princeton, New Jersey.

APPENDIX

Simulations were performed at constant particle number, volume, and temperature (N,V,T). The equations of motion were integrated via a Verlet scheme[26]

$$\mathbf{r}(t+\Delta t) = 2\mathbf{r}(t) - \mathbf{r}(t-\Delta t) + \frac{\mathbf{F}(t)}{m}(\Delta t)^2 + O(\Delta t^4), \tag{A1}$$

where $\mathbf{r}$ is the particle's position m, its mass, and $\mathbf{F}$, the force on the particle. All interactions were truncated at 2.8σ (or $2.8\sigma_2$ in mixture simulations, with 2 denoting the solvent). Thermostatting was implemented by application of Gauss' principle of least constraints[29,30] whereby the force on each particle is the sum of two terms

$$\mathbf{F} = \mathbf{F}^{(u)} + \mathbf{F}^{(c)}, \tag{A2}$$

where superscripts u and c denote unconstrained and constraint-imposing forces, respectively. The former are the usual conservative forces arising from the interparticle potential, the latter constrain the total kinetic energy, forcing it to remain constant. If, in the spirit of Gauss' principle of least constraints, we demand that the actual, constrained trajectories be such that they deviate as little as possible (in a least-squares sense) from the unconstrained trajectories,[30] we obtain, for the constrain-imposing force on particle i,

$$\mathbf{F}_i^{(c)} = -m_i\dot{\mathbf{r}}_i\left(\sum_{i=1}^{N}\dot{\mathbf{r}}_i\cdot\mathbf{F}_i^{(u)}\right)\Big/\left(\sum_{i=1}^{N}m_i\dot{\mathbf{r}}_i^2\right) \quad (i=1,\ldots,N). \tag{A3}$$

Velocities were explicitly computed from the scheme

$$\dot{\mathbf{r}}(t+\Delta t) = \dot{\mathbf{r}}(t-\Delta t) + 2\Delta t\frac{\mathbf{F}}{m} + O(\Delta t^3). \tag{A4}$$

Unconstrained forces and potentials were tabulated, with the interval $0 < r < r_c$ divided into 10 000 equally spaced increments. Force calculations were done via the implementation of the diagonal algorithm due to Brode and Ahlrichs.[31] The time step Δt was set at 2.5×10^{-4}, in units of $l\sqrt{m/\epsilon}$ (or $l\sqrt{m_1/\epsilon_2}$ in mixture simulations, with 1 denoting the solute, and 2, the solvent; l is the length of the periodic box). Simulations of the attractive mixture at state points A and C employed a time step of $2\times10^{-4}\ l\sqrt{m_1/\epsilon_2}$.

Simulations with 500, 864, 1372, and 2048 identical particles at state point B were performed in order to select a system size large enough as to guarantee that the correlation length be smaller than $l/2$. The pair correlation function decayed to 1 within $l/2$ for $N \geqslant 864$. Furthermore, the calculated curves (i.e., g_{22}) were indistinguishable for $N \geqslant 864$. We therefore adopted $N = 864$ as our system size for all simulations.

We now outline the van der Waals theory calculations for the repulsive and attractive mixtures. In the first place, we write the identities[6–8]

Downloaded 20 Jul 2006 to 128.112.35.75. Redistribution subject to AIP license or copyright, see http://jcp.aip.org/jcp/copyright.jsp

$$\overline{V}_1^{\infty}\rho = \delta K_T, \tag{A5}$$

$$\xi = (\rho kT - \delta)K_T, \tag{A6}$$

where $\overline{V}_1^{\infty}$ is the solute's partial molar volume at infinite dilution in a binary mixture, ρ is the solvent's number density, K_T its isothermal compressibility, ξ is the cluster size (defined as the excess number of solvent molecules surrounding infinitely dilute solute molecules with respect to a uniform distribution at bulk conditions), and δ is the infinite dilution limit of the rate of change of pressure upon solute addition at constant solvent mass, temperature and volume, multiplied by the number of molecules (N) in the volume under consideration (V),

$$\delta = \lim_{N_1/N_2 \to 0}\left[N\left(\frac{\partial P}{\partial N_1}\right)_{T,V,N_2}\right]. \tag{A7}$$

Equations (A5) and (A6) are of general validity, and show that, in near-critical systems, both $\overline{V}_1^{\infty}$ and ξ scale as K_T, with signs given by those of δ and $(\rho kT - \delta)$, respectively (note that in an ideal gas mixture, $\delta = \rho kT$, and hence, of course, $\overline{V}_1^{\infty} = kT/P$, $\xi = 0$). If $\delta < 0$, then in near-critical systems, $\overline{V}_1^{\infty} \to -\infty$, $\xi \to \infty$ (attractive behavior); if $0 < \delta < \rho kT$, then $\overline{V}_1^{\infty} \to \infty$, $\xi \to \infty$ (weakly attractive behavior); if $\delta > \rho kT$, then $\overline{V}_1^{\infty} \to \infty$, $\xi \to -\infty$ (repulsive behavior). It follows from Eqs. (A5)–(A7) that, for a van der Waals near-critical mixture with Lorentz–Berthelot combining rules,[8] the necessary and sufficient condition for attractive behavior is

$$\gamma < \frac{3(3-\rho_r)^2}{4}\cdot\frac{\alpha^{1/2}}{T_r} + \left(1 - \frac{3}{\rho_r}\right) \tag{A8}$$

whereas, for repulsive behavior, we want

$$\gamma > \frac{3(3-\rho_r)^2}{4}\cdot\frac{\alpha^{1/2}}{T_r} + \left(\frac{\rho_r}{3} - 1\right), \tag{A9}$$

where $\gamma = b_1/b_2$, $\alpha = a_1/a_2$ (van der Waals parameters), and ρ_r, T_r are the solvent's reduced density and temperature. Then, since $3b = \rho_c^{-1}$ and $8a = 27bkT_c$ for a van der Waals fluid, we have, for Xe in Ne,

$$\gamma = 2.726, \tag{A10}$$

$$\alpha = 17.769, \tag{A11}$$

and, for Ne in Xe

$$\gamma = 0.3668, \tag{A12}$$

$$\alpha = 0.05628. \tag{A13}$$

Therefore, along the critical isochore, and for $T_r = 1.037$ (state point B), the right-hand sides of inequalities (A8) and (A9) equal 10.195 and 0.01964, respectively. In the light of Eqs. (A10) and (A12) we conclude that, within the framework of the van der Waals–Lorentz–Berthelot theory, mixture 1 (Xe in Ne) is indeed attractive, and mixture 2 (Ne in Xe), repulsive.

[1] C. A. Eckert, D. H. Ziger, K. P. Johnston, and T. K. Ellison, Fluid Phase Eq. **14**, 167 (1983).
[2] C. A. Eckert, D. H. Ziger, K. P. Johnston, and S. Kim, J. Phys. Chem. **90**, 2738 (1986).
[3] S. Kim and K. P. Johnston, Ind. Eng. Chem. Res. **26**, 1206 (1987).
[4] S. Kim and K. P. Johnston, AIChEJ **33**, 1603 (1987).
[5] J. F. Brennecke and C. A. Eckert, *Proc. Int. Symp. on Supercritical Fluids (Nice, France)*, edited by M. Perrut (1988), p. 263.
[6] P. G. Debenedetti, Chem. Eng. Sci. **42**, 2203 (1987).
[7] P. G. Debenedetti and S. K. Kumar, AIChEJ **34**, 645 (1988).
[8] P. G. Debenedetti and R. S. Mohamed, J. Chem. Phys. **90**, 4528 (1989).
[9] H. D. Cochran, L. L. Lee, and D. M. Pfund, Fluid Phase Eq. **39**, 161 (1988).
[10] A. M. Rozen, Russ. J. Phys. Chem. **50**, 837 (1976).
[11] H. D. Cochran, D. M. Pfund, and L. L. Lee, *Proc. Int. Symp. on Supercritical Fluids (Nice, France)*, edited by M. Perrut (1988), p. 245.
[12] H. D. Cochran and L. L. Lee, AIChEJ **34**, 170 (1988).
[13] I. R. Krichevskii, Russ. J. Phys. Chem. **41**, 1332 (1967).
[14] J. C. Wheeler, Ber. Bunsenges. Phys. Chem. **76**, 308 (1972).
[15] J. M. H. Levelt Sengers, Fluid Phase Eq. **30**, 31 (1986).
[16] J. M. H. Levelt Sengers, G. Morrison, and R. F. Chang, Fluid Phase Eq. **14**, 19 (1983).
[17] J. M. H. Levelt Sengers, G. Morrison, G. Nielson, R. F. Chang, and C. M. Everhart, Int. J. Thermophys. **7**, 231 (1986).
[18] J. M. H. Levelt Sengers, C. M. Everhart, G.Morrison, and K. Pitzer, Chem. Eng. Commun. **47**, 315 (1986).
[19] J. M. H. Levelt Sengers, R. F. Chang, and G. Morrison, in *Equations of State: Theory and Applications*, edited by K. C. Chao and R. L. Robinson, *ACS Symp. Ser. No. 300* (American Chemical Society, Washington, D.C., 1986), p. 110.
[20] J. V. Sengers and J. M. H. Levelt Sengers, Ann. Rev. Phys. Chem. **37**, 189 (1986).
[21] R. F. Chang and J. M. H. Levelt Sengers, J. Phys. Chem. **90**, 5921 (1986).
[22] R. F. Chang, G. Morrison, and J. M. H. Levelt Sengers, J. Phys. Chem. **88**, 3389 (1984).
[23] R. C. Reid, J. M. Prausnitz, and B. Poling, *The Properties of Gases and Liquids*, 4th edition (McGraw–Hill, New York, 1987), p. 733.
[24] D. W. Matson, J. L. Fulton, R. C. Petersen, and R. D. Smith, Ind. Eng. Chem. Res. **26**, 2298 (1987).
[25] S. K. Kumar, U. W. Suter, and R. C. Reid, Fluid Phase Eq. **29**, 373 (1986).
[26] L. Verlet, Phys. Rev. **159**, 98 (1967).
[27] T. L. Hill, J. Chem. Phys. **23**, 617 (1955).
[28] E. M. Sevick, P. A. Monson, and J. M. Ottino, J. Chem. Phys. **88**, 1198 (1988).
[29] K. F. Gauss, J. Reine Angew. Math. **IV**, 232 (1829).
[30] D. J. Evans, W. G. Hoover, B. H. Failor, B. Moran, and A. J. C. Ladd, Phys. Rev. A **28**, 1016 (1983).
[31] S. Brode and R. Ahlrichs, Comp. Phys. Commun. **42**, 51 (1986).

Downloaded 20 Jul 2006 to 128.112.35.75. Redistribution subject to AIP license or copyright, see http://jcp.aip.org/jcp/copyright.jsp